Tunneling studies of two-dimensional states in semiconductors with inverted band structure: Spin-orbit splitting and resonant broadening

G. M. Minkov, A. V. Germanenko, V. A. Larionova, and O. E. Rut
Institute of Physics and Applied Mathematics, Ural University, Ekaterinburg 620083, Russia
(Received 16 January 1996)

The results of tunneling studies of the energy spectrum of two-dimensional (2D) states in a surface quantum well in a semiconductor with inverted band structure are presented. The energy dependence of quasimomentum of the 2D states over a wide energy range is obtained from the analysis of tunneling conductivity oscillations in a quantizing magnetic field. The spin-orbit splitting of the energy spectrum of 2D states, due to inversion asymmetry of the surface quantum well, and the broadening of 2D states at the energies, when they are in resonance with the heavy hole valence band, are investigated in structures with different strengths of the surface quantum well. A quantitative analysis is carried out within the framework of the Kane model of the energy spectrum. The theoretical results are in good agreement with the tunneling spectroscopy data. [S0163-1829(96)07324-9]

I. INTRODUCTION

A specific feature of a semiconductor with inverted energy band structure is the absence of an energy gap between conduction and valence bands. These bands are the two branches of the fourfold Γ_8 band. The states of the Γ_8 band are classified by the projection of the angular momentum $J=3/2$ onto the direction of quasimomentum k. The states with a projection of $\pm 1/2$ are conduction band states, hereafter referred to as the spin states of an electron. The Γ_6 band, which is a conduction band in ordinary semiconductors A^3B^5 and A^2B^6 with an open gap, is the light hole band, and lies below the degeneracy point for the energy difference $E_g = E^{\Gamma_6} - E^{\Gamma_8}$.

Such peculiarities of the band structure of inverted semiconductors lead to some special features of the energy spectrum of spatially confined systems, based on these semiconductors. Thus, it was predicted theoretically[1] that so-called interface two-dimensional (2D) states can exist near the boundary of an inverted semiconductor even without an attractive electrostatic potential. It was shown in a number of theoretical and experimental articles[2–8] that these states play a key part in forming the energy spectrum of 2D states in heterostructures and superlattices based on inverted semiconductors.

The absence of a forbidden gap in the inverted semiconductors leads to the fact that at negative energies (hereafter we measure energy from the degeneracy point of the Γ_8 band in the volume) the 2D states in the surface quantum well are resonant with the heavy hole valence band and, therefore, broadening should be present in this energy range. Such effects have been discussed for narrow gap semiconductors. However, in these materials, 2D electron states at energies less than the energy of the top of the valence band are separated from the heavy and light hole states by a barrier and the width of this barrier is proportional to the forbidden gap. So, the effect of the resonance broadening in ordinary semiconductors should differ from that in gapless semiconductors.

Of special interest are 2D systems in asymmetric quantum wells. The lack of inversion symmetry in this case leads to the spin splitting of the 2D subbands at $k \neq 0$ due to spin-orbit coupling even without a magnetic field. This phenomenon for 2D electron states has been studied extensively in semiconductors with $E_g > 0$.[9–14] In such materials the conduction band is the twofold degenerate Γ_6 band and the spin-orbit interaction can be taken into account within perturbation theory.[14] As mentioned above, in inverted semiconductors the conduction band is one of branches of the Γ_8 band and the spin-orbit coupling has been considered from the onset.[15]

This work is devoted to the investigation of the energy spectrum of 2D states in the surface quantum well in the inverted semiconductor $Hg_{1-x}Cd_xTe$ using tunneling spectroscopy in a quantizing magnetic field. This method was used for the first time in an investigation of the 2D states in an InAs surface accumulation layer by Tsui in Ref. 16. Since then, 2D states in a large variety of semiconductors, e.g., GaAs,[17] InSb,[18] and InAs,[19] were studied by tunneling spectroscopy in a magnetic field. However, there are only a few tunneling experiments on structures based on inverted semiconductors.[8,20]

Unlike traditional methods (galvanomagnetic phenomena, volt-capacitance experiments), which give information about the carriers at the Fermi energy, this method allows one to obtain information about the energy dependence of the quasimomentum of carriers over a wide range of energies, both for empty and occupied states. In this work we have also used a refinement of tunneling spectroscopy that allowed us to investigate 2D states at energies, which are given by the applied bias, for different quantum well strengths.

In the present article, in contrast to previous publications,[8,20] we report on results obtained on tunnel structures with a larger strength of the surface potential well. The preparation of such tunnel structures has been made possible by the use of Yb as a metal electrode, which has a low work function. This allows us to observe both spin branches, which are split by the spin-orbit interaction, and 2D states at large negative energies where they are in resonance with the valence band.

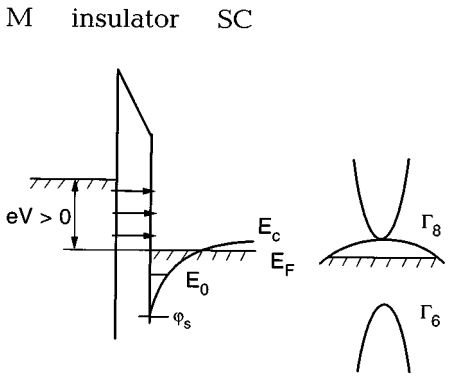

FIG. 1. Energy diagram of a metal (M)-insulator–inverted-semiconductor (SC) tunnel junction with a surface quantum well for a bias $V>0$.

The article is organized as follows. In Sec. II some features of the tunneling spectroscopy of 2D states in a quantizing magnetic field are considered. The experimental details and innovations in the tunneling spectroscopy method are given in Sec. III. In Sec. IV, experimental results obtained for the tunnel structures with different strengths of the surface potential well are presented and analyzed. Section V is devoted to the theoretical description of the energy spectrum of 2D states in a surface quantum well of an inverted semiconductor. The basic equations used in the calculations of resonant 2D states are spelled out. A comparison between experiment and theory is discussed in Sec. VI, and, finally, conclusions are made in Sec. VII.

II. OSCILLATIONS OF THE TUNNELING CONDUCTIVITY IN A MAGNETIC FIELD

In principle, the bias dependence of the tunneling conductivity of a metal-insulator–semiconductor structure contains information on the energy spectrum of both 3D and 2D states that may exist in the surface quantum well of the semiconductor. The investigations of tunneling conductivity oscillations in a magnetic field permit one to obtain the most reliable information on the energy spectrum, because in this case it is possible to determine directly the positions of the Landau levels and energy intervals between them.

Different types of oscillations of the tunneling conductivity may occur in the metal-insulator–semiconductor structure with 2D states localized in the surface quantum well (Fig. 1). The tunneling current in such a structure is the sum of the current due to tunneling to 2D (j_{2D}) and to 3D (j_{3D}) states. The oscillations of $\sigma_{3D}\equiv dj_{3D}/dV$ versus magnetic field and bias have been considered earlier.[21–23] The maxima in σ_{3D} occur when the metal Fermi level is aligned with one of the bulk Landau levels of the semiconductor. These oscillations are periodic in the reciprocal magnetic field with the period

$$\Delta(E_F+eV)=\frac{2\pi e}{c\hbar S(E_F+eV)}, \tag{1}$$

where E_F is the semiconductor Fermi energy and $S(E_F+eV)$ is the extreme cross section of the isoenergy surface at the energy E_F+eV. In semiconductors with an isotropic spectrum $S(E)=\pi k^2(E)$. This gives one the opportunity to determine the energy dependence of the quasimomentum for the bulk states over a wide energy range.[22,23]

The tunneling current to 2D states at bias V, magnetic field B, and temperature $T=0$ is

$$j_{2D}(V)=\int_{E_F}^{E_F+eV} g_{2D}(E-E_0,B)D(E,V)dE, \tag{2}$$

where $g_{2D}(E-E_0,B)$, E_0, $D(E,V)$ stand for the density of 2D states, the energy of the bottom of the 2D subband, and the barrier tunneling transparency, respectively. An applied voltage not only shifts the Fermi quasilevels of the metal and semiconductor relative to each other but also changes the surface quantum well (and therefore E_0) and barrier transparency as well. Thus the tunneling conductivity for tunneling to 2D states is

$$\begin{aligned}\sigma_{2D}&\equiv\frac{dj_{2D}}{dV}\\ &=g_{2D}(E-E_0,B)D(E,V)\big|_{E_F+eV}\\ &\quad+\int_{E_F}^{E_F+eV}\left(\frac{dg_{2D}(E-E_0,B)}{dV}D(E,V)\right.\\ &\quad\left.+g_{2D}(E-E_0,B)\frac{dD(E,V)}{dV}\right)dE.\end{aligned} \tag{3}$$

To a first approximation, the variation of $g_{2D}(E-E_0,B)$ with bias is due to changes in E_0, and relationship between E_0 and V is linear, i.e. $E_0(V)=E_0(0)+\alpha V$ and $g_{2D}(E-E_0,B)=g_{2D}(E-E_0(V),B)$. This results in the expression

$$\begin{aligned}\sigma_{2D}&=D(E,V)g_{2D}[E-E_0(V),B]\big|_{E_F+eV}\\ &\quad+\alpha\overline{D(V)}g_{2D}[E-E_0(V),B]\big|_{E_F+eV}\\ &\quad-\alpha\overline{D(V)}g_{2D}[E-E_0(V),B]\big|_{E_F}\\ &\quad+\int_{E_F}^{E_F+eV}g_{2D}[E-E_0(V),B]\frac{dD(E,V)}{dV}dE,\end{aligned} \tag{4}$$

where $\overline{D(V)}$ is the mean value of $D(E,V)$. A magnetic field $B\|n$ (n is the normal to the surface) quantizes the energy spectrum of 2D states and g_{2D} becomes an oscillatory function of B and E. One can see from expression (4) that two types of conductivity oscillation should occur in a magnetic field.

(i) In the first type, oscillations arise whenever a Landau level of 2D states is aligned with the energy E_F+eV [the first and the second terms in Eq. (4)]. If the surface potential depends only slightly on V, then the positions of these oscillations allow one to immediately determine the energy spectrum of the 2D states by the same procedure as for 3D states [see Eq. (1)]. As $B\to 0$ the fan chart of these oscillations is extrapolated to the energy of the bottom of the 2D subband.

(ii) In the second type, oscillations appear whenever a Landau level of the 2D states is aligned with the energy E_F [the third term in Eq. (4)]. As $B\to 0$ the fan chart of these oscillations is extrapolated to the bias at which the 2D carriers (but not states) disappear, i.e., to the bias for which the

TABLE I. Parameters of investigated structures.

Structure	x	E_g (meV)	m_n ($10^2 m_0$)	N_A-N_D (10^{17} cm^{-3})	E_F (meV)	φ_s (meV)[a]	L (10^{-6}cm)[a]
10-1	0.125	-70 ± 5	6.25	60	-15 ± 5	275 ± 5	1.0
10-2	0.125	-70 ± 5	6.25	60	-15 ± 5	270 ± 5	1.0
10-3	0.125	-70 ± 5	6.25	60	-15 ± 5	240 ± 5	0.95
10-4	0.125	-70 ± 5	6.25	60	-15 ± 5	230 ± 5	0.92
10-5	0.125	-70 ± 5	6.25	60	-15 ± 5	210 ± 5	0.88
10-6	0.125	-70 ± 5	6.25	60	-15 ± 5	180 ± 5	0.8
11-1	0.115	-90 ± 5	8.0	20	-10 ± 5	200 ± 5	1.5
12-1	0.105	-110 ± 5	9.75	8	-8 ± 3	275 ± 5	2.75
13-7	0.095	-125 ± 5	11.5	5	-5 ± 2	260 ± 5	2.85

[a]The values are given for $V=80$ mV for the 10-1 to 11-1 structures, and for $V=0$ mV for other structures.

bottom of the 2D subband becomes higher than the semiconductor Fermi level. The amplitude of these oscillations is proportional to the rate of variation of E_0 with bias (α). When $\alpha=0$ or $E_0>E_F$, these oscillations are absent and only oscillations of the first type will be observed.

We are not concerned with oscillations of the fourth term in Eq. (4), because an oscillating function is an integrand, and, therefore, the amplitude of oscillations of this term is small.

Up to now we have not considered possible oscillations of $D(E,V)$ in a magnetic field. The effects of these oscillations might be dominant in tunnel structures with a monocrystal barrier. For such a barrier the decay constant of the wave function in an insulator is rigidly determined by the energy. Therefore, small oscillations of the surface potential φ_s (Fig. 1) give rise to significant oscillations of $D(E,V)$. Oscillations of φ_s as well as oscillations of the third term in Eq. (4) occur whenever a Landau level of the 2D states is aligned with the energy E_F.[16] An analysis of the expression (3) shows that the second type of oscillations will be predominantly observed in such structures. We believe that the oscillations of this kind were observed in HgTe/$Hg_{1-x}Cd_xTe$ heterostructures.[24]

III. EXPERIMENTAL DETAILS

The differential conductivity $\sigma_d=dj/dV$ as a function of bias and magnetic field in metal-insulator $Hg_{1-x}Cd_xTe$ ($0.08<x<0.13$) structures was investigated in magnetic fields up to 6 T at the temperature of 4.2 K. Tunnel junctions were fabricated on monocrystalline p-$Hg_{1-x}Cd_xTe$ with the concentration of uncompensated acceptors $N_A-N_D=(2.5-60)\times10^{17}\text{cm}^{-3}$. The doping level was determined from an analysis of galvanomagnetic phenomena in the temperature range 1.5–70 K. Ultraviolet illumination for 5–15 min in dry air was used to form a thin oxide, which served as a tunneling barrier. Then a metallic electrode (Yb) was evaporated through a mask. Several tunnel contacts prepared on each sample were investigated. The parameters of the tunnel structures are listed in the Table I. It is assumed that the surface electric field in these structures arises from the work function difference of Yb and the semiconductor.[25]

The resistance of our structures is 0.1–1 kΩ and is determined mainly by the barrier transparency because the resistance associated with the transition of electrons between 2D and bulk states of the semiconductor is significantly less in metal-insulator–semiconductor structures based on inverted semiconductors.

The traditional modulation procedure was used for measuring the differential conductivity and its derivative $d\sigma/dV$. In some cases a refined method was used.[26] In parallel with a small (about 1 mV) alternative voltage with frequency $f=670$ Hz and direct bias V, impulses with a period $T\gg1/f$ and duration $t\ll1/f$ were imposed across the tunnel contact (Fig. 2). These impulses lead to a change in the electric charge of the localized states which occur in the insulator or at the insulator-semiconductor boundary. If the relaxation time of these states far exceeds T, these impulses result in an increase or decrease (depending on sign of the impulses) of the strength of the surface potential well. Thus, measurements taken during the interval between impulses make it possible to get information about the energy spectrum of the 2D states with energy E_F+eV but for a different strength of the surface potential well.

IV. EXPERIMENTAL RESULTS

Let us consider first the results obtained from the measurements of the tunnel structures prepared on the most heavily doped sample (Table I). The oscillation curves for such structures are simpler and therefore easier to interpret. Typical magnetic field dependences of the oscillatory part of the derivative of the tunneling conductivity with respect to voltage at different biases are presented in Fig. 3. Oscilla-

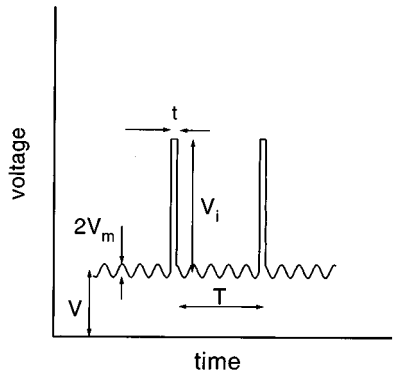

FIG. 2. Voltage which is applied to a tunnel junction. The voltage is a sum of a dc bias V, an ac modulation voltage with amplitude V_m, and impulses with amplitude V_i.

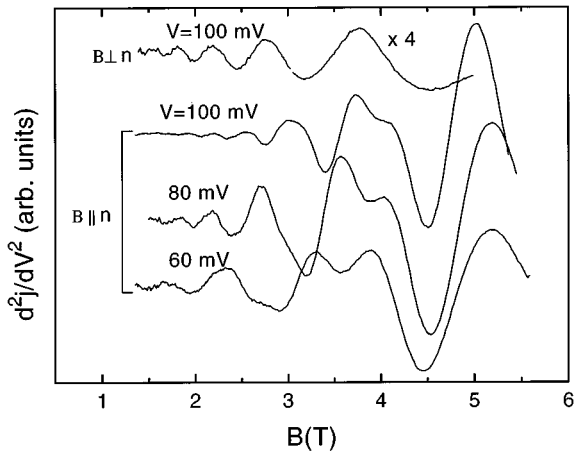

FIG. 3. d^2j/dV^2 versus B curves at different biases for the structure 10-1.

tions are observed for both orientations of magnetic field, $B\|n$ and $B\perp n$. The positions of the maxima of d^2j/dV^2 for $B\|n$ in the B, V coordinates are plotted in Fig. 4. It is clear that with $B\|n$, every oscillation curve in Fig. 3 is a convolution of several components and therefore it is difficult to follow the maxima positions of each component in Fig. 4. For better distinction a Fourier transformation of the oscillation curves is carried out. As shown in Fig. 5 for $B\perp n$ there is only one fundamental field and for $B\|n$ two fundamental fields occur in the oscillation curves (a shoulder, whose position coincides with the maximum position at $B\perp n$, is resolved at some biases). Now one can separate each component peak, take the inverse Fourier transform, and follow the positions of the oscillation maxima of any one of the oscillation components independently. The curves in Fig. 4 were obtained in this way and it can be seen that they adequately describe all the experimental data.

As mentioned above [Eq. (1)] the period of oscillations $\Delta = B_f^{-1}$ is determined by the value of quasimomentum. Bias dependences of k for both orientations of magnetic field are plotted in Fig. 6.

For $B\perp n$, the spectrum of 2D states is not quantized by

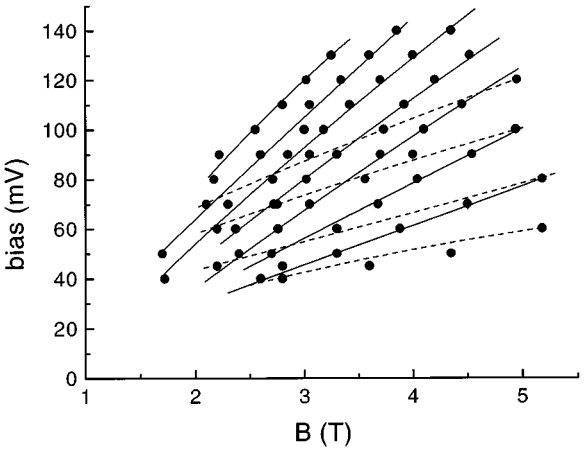

FIG. 4. The positions of the maxima of the d^2j/dV^2 versus B curves for the structure 10-1 for $B\|n$. The curves are obtained in the way described in the text.

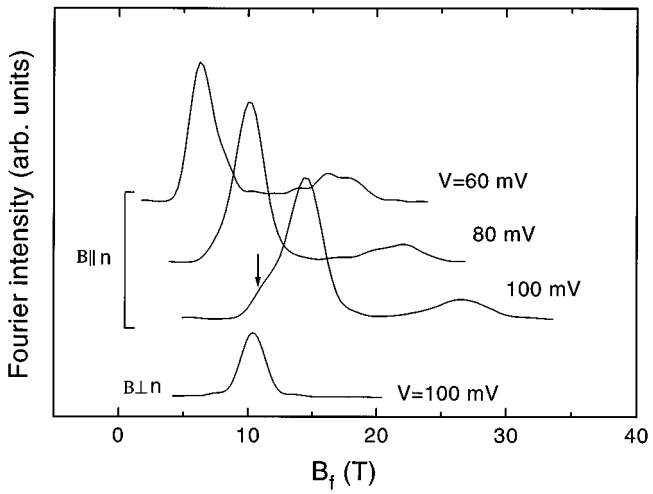

FIG. 5. The results of Fourier transformation of the tunneling curves plotted in Fig. 3. A shoulder on a low-field peak for a bias of 100 mV for $B\|n$ corresponds to tunneling to the bulk Landau levels.

the magnetic field and, therefore, the oscillations of the tunneling conductivity are due to tunneling to Landau levels of bulk states only. Hence, open circles in Fig. 6 correspond to the energy spectrum of the bulk states. The experimental data are in good agreement with the $E(k)$ dependence calculated within the Kane model. Therefore using parameters $P = 8\times10^{-8}$ eV cm, $\Delta_0 = \infty$ (where Δ_0 is the energy difference between valence band Γ_8 and split-off Γ_7 band) we determined the values of E_g and the effective mass on the bottom of the conduction band m_n for all the structures (Table I). Extrapolation of this curve to $k=0$ gives the semiconductor Fermi energy $E_F = -eV_0$ (Fig. 6), which is also given in the Table I.

For $B\|n$, oscillations are connected mainly with tunneling to 2D states localized in the surface quantum well of the

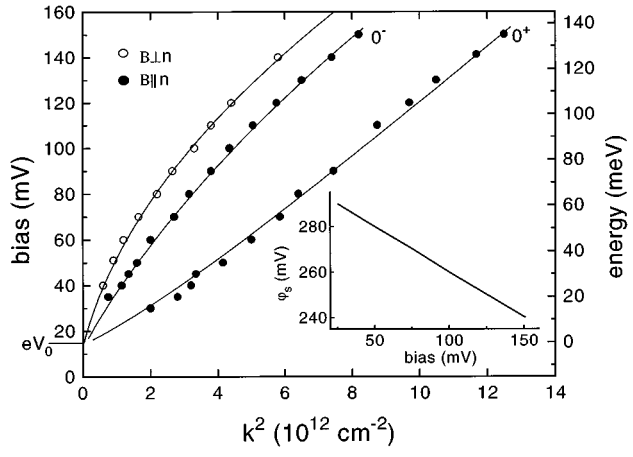

FIG. 6. Bias dependences of k^2 for the structure 10-1. Open and full circles represent the experimental data for $B\perp n$ and $B\|n$, respectively. The upper curve is the dispersion law of the bulk electrons, calculated in the framework of the Kane model with parameters $E_g = -70$ meV, $P = 8\times10^{-8}$ eV cm. The other curves are the result of theoretical calculations for the 2D states described in Sec. V. The inset shows the bias dependence of φ_s.

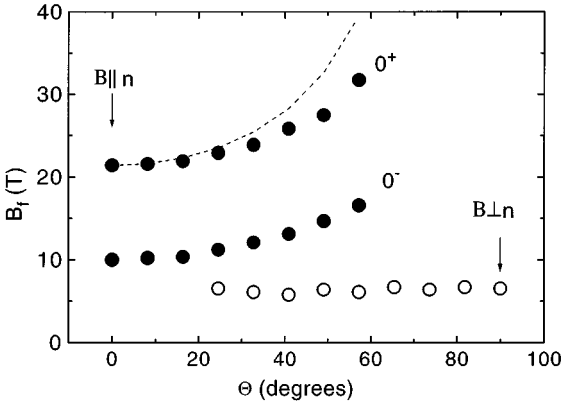

FIG. 7. Angular dependence of fundamental magnetic fields for the structure 10-1, measured at $V=80$ mV. Dashed line indicates the $\cos(\Theta)^{-1}$ dependence. Open and full circles relate to tunneling to the bulk and 2D states, respectively.

semiconductor. This is evident from the typical angular dependence of the fundamental fields (Fig. 7). The reasons for some deviation from the classical angle dependence $B(\Theta)=B(0)/\cos(\Theta)$, where Θ is the angle between B and n, were discussed in Ref. 20. At $\Theta>20°$ the Θ-independent maximum, which results from tunneling to bulk Landau levels, is resolved in the Fourier transform (open circles in Fig. 7). Thus, Fig. 6 shows that two branches of 2D states exist in this structure and at $k\rightarrow 0$ they are extrapolated to the bias $V_0>0$. This means that there are no 2D states below the Fermi level, i.e., 2D electrons are absent and therefore only oscillations of the first type (see Sec. II) can be observed.

There are two possibilities for the explanation of these two branches; they are the ground and excited subbands of 2D states or they are two branches of the ground subband split by the spin-orbit interaction in the asymmetric quantum well. An estimation of the difference between the energies of the ground and excited subbands at $k=0$ shows that for structures based on a heavily doped semiconductor with a small effective mass (see Table I) this value should be more than 50–100 meV (a comparison will be given in more detail in Sec. VI). This value far exceeds the experimental one (Fig. 6). Thus two branches of the 2D states in structure 10-1 (Fig. 6) correspond to two different spin branches of the ground subband which is split by spin-orbit interaction. Hereafter supercripts + and − refer to different spin branches. Analogous experimental results have been obtained for the 11-1 structure.

The structure 10-1 was also measured with voltage impulses which change the surface potential (see preceding section) and shift the 2D branches relative to the bulk states. Figure 8 shows this shift at $V=80$ mV versus the amplitude of the impulses. The distances between the branches of the 2D states and bulk states $\Delta(k^{+,-})^2=(k^{+,-})^2-k^2_{\rm bulk}$ versus quasimomentum of the lower branch of the 2D state $(k^+)^2$ are plotted in Fig. 9. The results for the 10-2 to 10-6 structures, which differ by the value of the surface potential, are also shown in Fig. 9. It can be seen that when $(k^+)^2$ decreases as the result of reduction in the surface potential, the upper branch of the 2D states is pushed into the continuum, i.e., these localized 2D states disappear, and for the 10-3 to

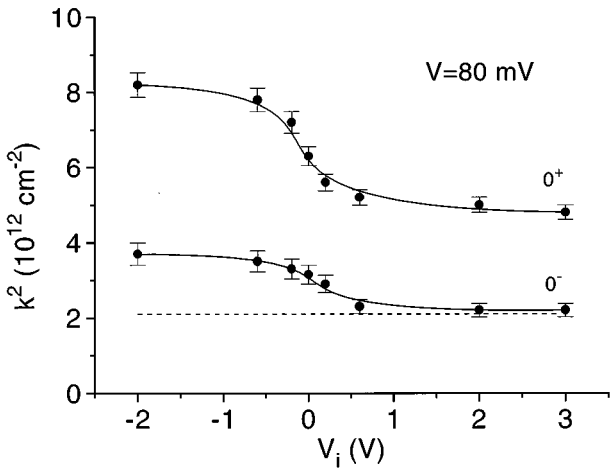

FIG. 8. A quasimomentum of 2D states as a function of the amplitude of impulses for a bias of $V=80$ mV, which corresponds to the energy $E=E_F+eV=65$ meV, for the structure 10-1. The dashed line shows the value of k^2 of the bulk electrons for the same energy. Solid curves are merely a guide for the eye.

10-6 structures, in which $\Delta(k^+)^2\leqslant 2\times 10^{12}\text{cm}^{-3}$, the only one k^+ branch of 2D states exists. The bias dependence of the quasimomentum of 2D states for one of these structures (structure 10-4) over all bias ranges is shown in Fig. 10.

The more complicated oscillation curves for $B\|n$ were observed for tunnel structures prepared on lesser doped samples. The maxima positions in V, B coordinates are plotted in Fig. 11 for structure 12-1 . An inspection of Fig. 11 shows that two main oscillation types are observed. The maxima of these oscillations shift in opposite directions relative to V as the magnetic field is varied. The behavior of the maxima positions with angle shows that both types of the

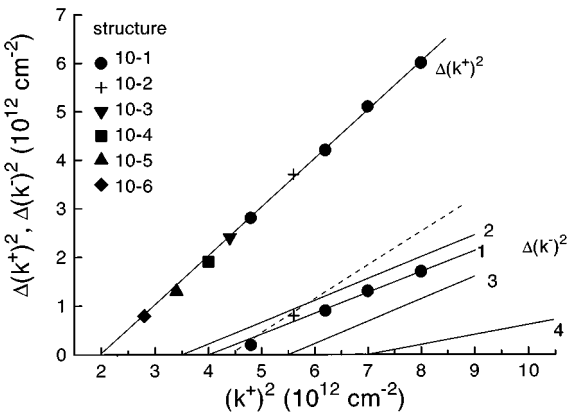

FIG. 9. The differences $\Delta(k^+)^2$ and $\Delta(k^-)^2$ as a function of $(k^+)^2$ for different structures, $V=80$ mV. Points for structure 10-1 have been obtained at different amplitudes of impulses. Solid curves are the result of numerical calculations carried out with parameters listed in the table and different band offset values: $D_c=2$ eV, $D_v=1$ eV for curve 1, $D_c=5$ eV, $D_v=1$ eV for curve 2, and $D_c=1$ eV, $D_v=1$ eV for curve 3. Curve 4 and the dashed curve are the results of exact and approximate (in accordance with Ref. 31) calculations with zero boundary conditions for the second component of the wave function. The upper curve is the same for the calculations with different parameters.

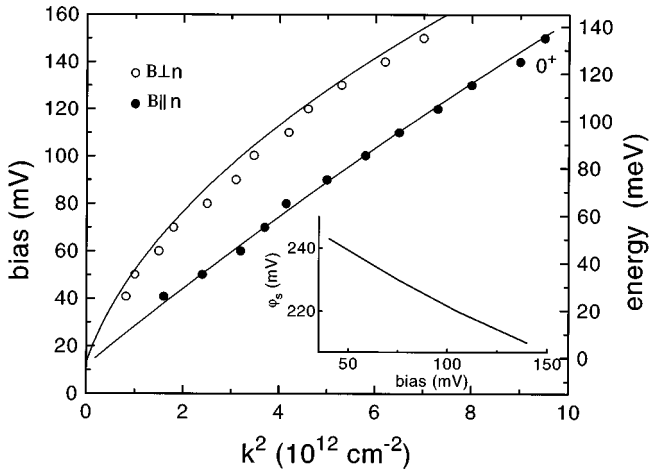

FIG. 10. Bias dependences of k^2 for structure 10-4. Open and full circles represent the experimental data for $B\perp n$ and $B\|n$, respectively. The upper curve is the dispersion law of the bulk electrons, calculated in the framework of the Kane model with parameters $E_g=-70$ meV, $P=8\times10^{-8}$ eV cm. The other curve is the result of theoretical calculations for the 2D states described in Sec. V. The inset shows the bias dependence of φ_s.

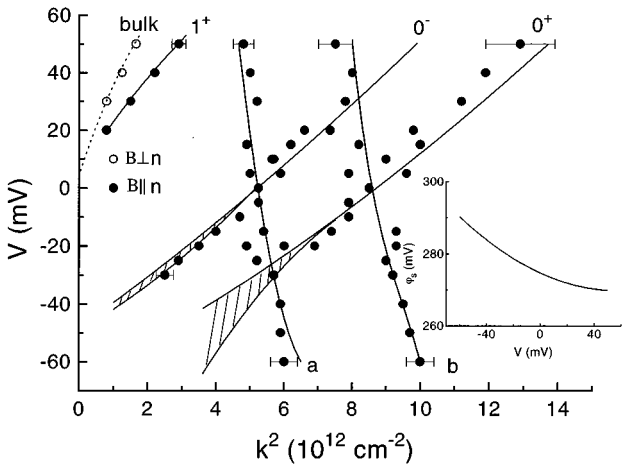

FIG. 12. The bias dependences of k^2 for structure 12-1. Symbols show the experimental data: the open and full circles correspond to the bulk and 2D states, respectively. The dotted curve is the dispersion law of the bulk electrons, calculated in the framework of the Kane model with parameters $E_g=-110$ meV and $P=8\times10^{-8}$ eV cm. The solid curves are the theoretical bias dependences of $k^2(E_F+eV)$ (curves 1^+, 0^+, and 0^-) and $k^2(E_F)$ (curves a and b). The inset shows the bias dependence of φ_s. The hatched regions show the broadening of the 2D energy levels.

oscillations are connected with 2D states. Taking the Fourier transform one can determine the fundamental fields, and using Eq. (1) one can calculate the quasimomentum of the states responsible for the oscillations at any bias (Fig. 12). The oscillations for $B\perp n$ as well as those for the structure 10-1 are due to tunneling to the Landau levels of the bulk states. Thus the open circles in Fig. 12 are the energy spectrum of the bulk states. The 1^+, 0^-, and 0^+ branches correspond to oscillations of the first type, i.e., to oscillations arising whenever the Landau levels of the 2D states coincide with the energy E_F+eV. The branches a and b relate to oscillations of the second type, i.e., to oscillations which arise whenever Landau levels of 2D states coincide with the energy E_F; therefore branches $0^+,b$ and $0^-,a$ intersect at $V=0$ (Fig. 12). The decrease of the quasimomentum at the energy $E=E_F$ with V (branches a,b) is a result of the decreasing concentration of 2D electrons due to a reduction of the depth of the surface potential well as bias is increased (inset in Fig. 12). We reason that two branches of the ground 2D subband, which is split by spin-orbit interaction, and one branch of the excited subband are observed for the structure 12-1 (Fig. 12). Such interpretation will be confirmed in Sec. VI. Both types of oscillations connected with tunneling into 2D states and analogous to Fig. 12, the bias dependence of the quasimomentum, were clearly observed in the structure 13-7 also.

It is significant that at negative biases up to $V=-30$ mV we observe oscillations of the first type, which occur whenever the Landau levels of 2D states coincide with the energy E_F+eV. At these energies the 2D states in the surface quantum well of the inverted semiconductor are in resonance with the valence band states. However, in spite of this fact broadening of the 2D states is not large enough to destroy the oscillation picture. To our knowledge, this is the first experimental observation of 2D states which lie significantly below the top of the valence band.

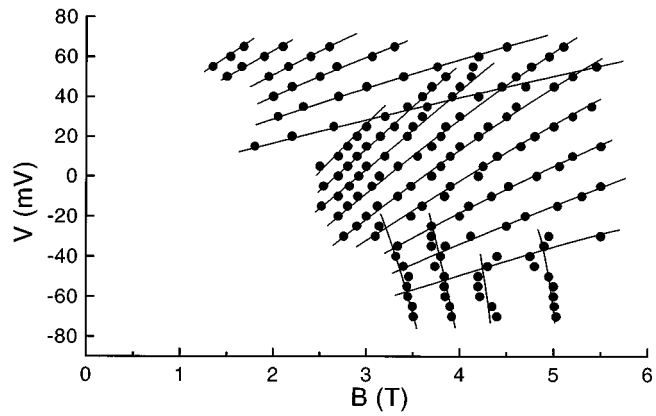

FIG. 11. Fan chart diagram for structure 12-1 at $B\|n$ orientation. The solid curves are merely a guide for the eye.

V. THEORETICAL MODEL

To describe the energy spectrum of 2D systems in wide gap semiconductors, the one-band approximation is usually used. In this case the energy spectrum is parabolic. Such an approach gives good results, because typical energies of 2D states in wide-gap systems are much less than the energy gap. In asymmetric quantum systems (e.g., in surface quantum wells), as a result of spin-orbit interaction, splitting of the energy spectrum arises even without an external magnetic field. It is common practice to interpret the experimental data in this case using the Bychkov-Rashba model.[9] The spin-orbit interaction is described here by one additional term, included in the dispersion law. It is linear in respect to quasimomentum, and contains a new parameter, which has to be calculated independently.

The one-band model is inapplicable in the case of 2D

states in narrow gap and inverted semiconductors. The strong interaction between the conduction and valence band makes it necessary to employ a multiband Hamiltonian in calculations of the energy spectrum of 2D systems. It is well known that the energy spectrum of A^2B^6 semiconductors can be described by the Kane Hamiltonian. Because the Dirac Hamiltonian, which is simpler for calculations, gives the same energy spectrum for electrons in the volume as the Kane Hamiltonian, the Dirac model is also widely used for calculations of the energy spectrum of 2D systems in such materials (see Refs. 11 and 27 and references therein). However, this is not quite correct. It was demonstrated in Ref. 4 that parameters of the energy spectrum of 2D electrons obtained with the Dirac and Kane models are radically different. The Kane model was used in our previous article on the energy spectrum of 2D electrons in $HgTe/Hg_{1-x}Cd_xTe$ heterostructures.[24] There are a number of points to be made before applying this model in calculations of the energy spectrum of 2D systems near the oxide-semiconductor interface.

There is difficulty in choosing the boundary conditions at the oxide-semiconductor interface, because the energy band structure of oxide is unknown. The interaction with remote bands is usually neglected in the Kane model, when it is used for finding the spectrum of 2D electron states. Then the Schrödinger equation is the system of ordinary differential equations, and traditional boundary conditions ($|\Psi|=0$ at the interface) lead in this approximation to the existence of a unique solution: the wave function is equal to zero over all space.[28]

One way out of this dilemma is to reduce the system of ordinary differential equations to one equation of second order which corresponds to one component of the wave function and to use zero boundary conditions only for this component.[10,29–31] This is a good approximation for 2D electron states in wide gap semiconductors, in which one component of the wave function is much greater than the other. However, all the components are of the same order of magnitude in narrow gap and inverted semiconductors, and additional arguments are needed as to why only one component has to go to zero at the semiconductor-oxide interface.

Another approach has been suggested by Sobkowicz in Ref. 28. Here, the assumption is made that the band structure of the insulator is similar to that of the semiconductor. The only difference is the value of the energy gap, which is much greater for an insulator than that for a semiconductor. Moreover, the condition $D_c, D_v \gg E$ (where D_c, D_v are conduction and valence band offsets, respectively) seems to be natural, because neither electrons nor holes have to be emitted from the semiconductor. Figure 13 presents schematically the model band structure for the case of inverted semiconductors. Because the electrostatic potential is constant at $z<-d$ and $z>L$, the exact wave functions are known in these regions. In this case the eigenvalue problem can be solved exactly using the techniques of direct numerical integration.[24]

Thus in the framework of this model one can understand which insulator parameters correspond to the zero boundary condition for the second component of the wave function (see expressions (7) and (9) which follow] used in Ref. 31. This can be understood from Fig. 14, which shows the calculated dependence of the energy of the ground 2D subband on the value of D_v, while the value of D_c is fixed (for details see Ref. 24). The splitting of the 2D subband into two branches 0^+ and 0^- results from spin-orbit interaction. It is clearly seen that the zero boundary condition used in Ref. 31 is a limiting case $D_v \to \infty$ and the limit is reached very slowly. The results obtained in the above model come close to the solution of the zero boundary condition problem only at $D_v > 100$ eV.

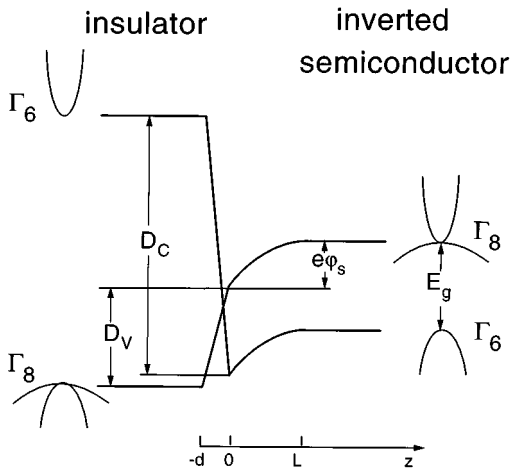

FIG. 13. Model of an insulator–inverted-semiconductor structure with a surface quantum well used in the calculations.

The approach discussed above neglects the interaction with remote bands which corresponds to infinite heavy hole mass. This is suitable for calculation of the energy spectrum of 2D electrons only for positive energies. When the energy of 2D states is negative, they are in resonance with the continuous spectrum of the heavy hole valence band. It is im-

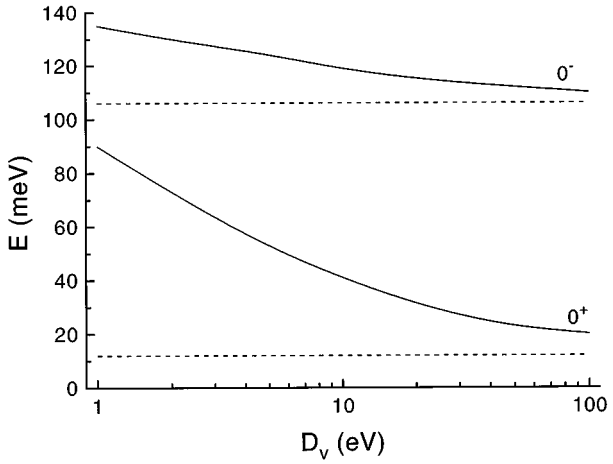

FIG. 14. The dependence of the energy of two branches of the 2D ground subband at $k=3\times10^6$ cm^{-1} on the valence band offset value while D_c is kept constant $D_c=1$ eV. The dashed lines are the energies of the branches calculated under zero boundary conditions for the second component of the wave function at the insulator–inverted-semiconductor interface. The calculations have been carried out with parameters $E_g=-70$ meV, $P=8\times10^{-8}$ eV cm, $N_A-N_D=6\times10^{18}$ cm^{-3}, $\varphi_s=240$ meV, and for parabolic surface quantum well.

portant to take remote bands into consideration in the calculation of the energy spectrum in this energy range, because the tunneling of the carriers from the space charge layer to the volume of a semiconductor can lead both to a change in the energy and a broadening of the 2D states.

To calculate the energy spectrum of 2D states taking remote bands into consideration, the usual assumption has been made, that the energy difference Δ_0 between the valence band Γ_8 and the split-off Γ_7 band is very large. In this case, the Kane Hamiltonian is a 6×6 matrix. We choose the direction z to be normal to the interface, and the direction of the carrier motion along y. Then the Hamiltonian can be block diagonalized into two 3×3 Hamiltonians for two groups of states. The Hamiltonian matrix for the first group is defined by

$$H^+=\begin{pmatrix} E^{\Gamma_6}+e\varphi(z) & i\sqrt{\frac{2}{3}}P\left(\frac{k_y}{2}-\frac{\partial}{\partial z}\right) & \frac{i}{\sqrt{2}}Pk_y \\ i\sqrt{\frac{2}{3}}P\left(-\frac{k_y}{2}-\frac{\partial}{\partial z}\right) & E^{\Gamma_8}+e\varphi(z) & \\ & -\frac{\hbar^2}{2m}\gamma_1\left(k_y^2-\frac{\partial^2}{\partial z^2}\right) & 0 \\ -\frac{i}{\sqrt{2}}Pk_y & 0 & E^{\Gamma_8}+e\varphi(z) \\ & & -\frac{\hbar^2}{2m}\gamma_1\left(k_y^2-\frac{\partial^2}{\partial z^2}\right) \end{pmatrix}, \tag{5}$$

where E^{Γ_6} and E^{Γ_8} are the energies of corresponding band edges, γ_1 is the parameter that describes the interaction with the remote bands, and $\varphi(z)$ is the electrostatic potential. The values P and γ_1 are assumed to be the same for both the semiconductor and insulator. The Hamiltonian H^- for the second group of states is obtained from H^+ by replacing k_y by $-k_y$. Thus, the Schrödinger equation

$$H^{\pm}\Psi=E^{\pm}\Psi \tag{6}$$

is a system of differential equations of second order, which determines two branches of the energy spectrum corresponding to two groups of states. The eigenvectors in the insulator and the volume of the semiconductor are known, because $\varphi(z)=\text{const}$ at $z<-d$ and $z>L$. There are two types of eigenvectors. The first type corresponds to a light particle and is

$$\Psi^{(l)}(k_y,k_z)=\begin{pmatrix} E+\gamma_1\frac{\hbar^2k^2}{2m}-E^{\Gamma_8} \\ \sqrt{\frac{2}{3}}P\left(k_z-\frac{ik_y}{2}\right) \\ \frac{i}{\sqrt{2}}Pk_y \end{pmatrix} e^{ik_yy+ik_zz} \tag{7}$$

where the energy for fixed k_y and k_z is obtained from the equation

$$(E-E^{\Gamma_6})\left(E-E^{\Gamma_8}+\frac{\gamma_1\hbar^2}{2m}(k_y^2+k_z^2)\right)=\tfrac{2}{3}P^2(k_y^2+k_z^2). \tag{8}$$

The second type corresponds to the heavy particle and is

$$\Psi^{(h)}(k_y,k_z)=\begin{pmatrix} 0 \\ -\frac{i}{\sqrt{2}}Pk_y \\ \sqrt{\frac{2}{3}}P\left(k_z+\frac{ik_y}{2}\right) \end{pmatrix} e^{ik_yy+ik_zz} \tag{9}$$

for the energy

$$E=E^{\Gamma_8}+\frac{\gamma_1\hbar^2}{2m}(k_y^2+k_z^2). \tag{10}$$

The wave function in the insulator Ψ_I can be written as a linear combination of $\Psi^{(h)}$ and $\Psi^{(l)}$,

$$\Psi_I=\Psi^{(h)}(k_y,-k_z^{(h)})+C\Psi^{(l)}(k_y,-k_z^{(l)}), \tag{11}$$

where C is some as yet unknown multiplier. Here only the terms that diminish at $z\to\infty$ are given.

In the region $z>L$ the wave function is given by

$$\Psi_{SC}=C_1\Psi^{(h)}(k_y,k_z^{(h)})+C_2\Psi^{(l)}(k_y,k_z^{(l)}) + C_3\Psi^{(h)}(k_y,-k_z^{(h)})+C_4\Psi^{(l)}(k_y,-k_z^{(l)}). \tag{12}$$

In Eqs. (11) and (12), $k_z^{(l)}$, $k_z^{(h)}$ stand for the quasimomentum components perpendicular to the interface, which for

any given k_y and E are determined from (8) and (10), respectively. Because only normalized solutions are of interest here, the coefficient C_4 in (12) has to be zero. So, we can now state the problem, which can be numerically calculated: at a fixed energy one needs to find a value of C for $z<-d$ such that subsequent numerical integration of the Schrödinger equation throughout the region of the potential results in a zero value for C_4.

The behavior of the potential $\varphi(z)$ in a semiconductor is determined from the Poisson equation for the charge density,

$$\rho(z)=-e|N_A-N_D|L\vartheta(L-z) \\ -e\sum \int_{E_i}^{E_F} g(E)|\Psi(E,z)|^2 dE, \qquad (13)$$

where the summation runs over all occupied 2D subbands. E_i denotes the energy of the bottom of the ith subband. The second term describes the contribution of the electrons localized in the quantum well. In the absence of 2D electrons (this situation occurs in the 10-1 to 11-1 structures), the second term in (13) is equal to zero, and the Poisson equation can be solved exactly. Then $\varphi(z)$ is parabolic,

$$\varphi(z)=\begin{cases}\varphi_s(1-z/L)^2, & 0\leqslant z\leqslant L \\ 0, & z>L,\end{cases} \qquad (14)$$

where

$$\varphi_s=\varphi(0), \quad L=\left(\frac{2\kappa\kappa_0\varphi_s}{e(N_A-N_D)}\right)^{1/2},$$

and κ is the dielectric constant. For the structures with a concentration of 2D electrons comparable to $(N_A-N_D)\times L$ (as in structures 12-1 and 13-7), one needs to calculate the potential self-consistently. We use here the assumption made in Ref. 24, namely, at the calculations of the charge density distribution we suppose that the wave function is energy independent $\Psi(E,z)=\Psi(E_F,z)$.

Let us now consider peculiarities of the 2D states resulting from resonance with the heavy hole band. All the results demonstrated in this section have been obtained with the following parameter values: $E_g=-110$ meV, $P=8\times10^{-8}$ eV cm, $\gamma_1=2$, $N_A-N_D=1\times10^{18}$ cm^{-3}, $\kappa=20$, and a parabolic dependence of $\varphi(z)$ with $\varphi_s=275$ mV. $D_c=2$ eV and $D_v=1$ eV are used (the choice of these values will be justified in the next section). The calculations show that the variation of the value of interface width d in the range 5-50 Å does not have a practical effect on the energy spectrum of 2D states.

Figure 15 shows the z dependence of $|\Psi(z)|^2$ for two energy values, corresponding to nonresonant ($E>0$) and resonant ($E<0$) 2D electron states. It is clearly shown that the wave function does not decay in the semiconductor region ($z>L$) at negative energies. This means that the charge carriers from the space charge layer may go into the volume of the semiconductor; its wave function is transformed from an electron into a heavy hole wave function in the process. To find the broadening of the 2D energy levels associated with such a resonance, one may turn to the scattering theory, namely, Levinson's theorem.[28,32]. This allows a calculation of a density of states, added to the valence band by the presence of the electrostatic potential $\varphi(z)$ and the semiconductor-insulator interface, treated as a scattering potential,

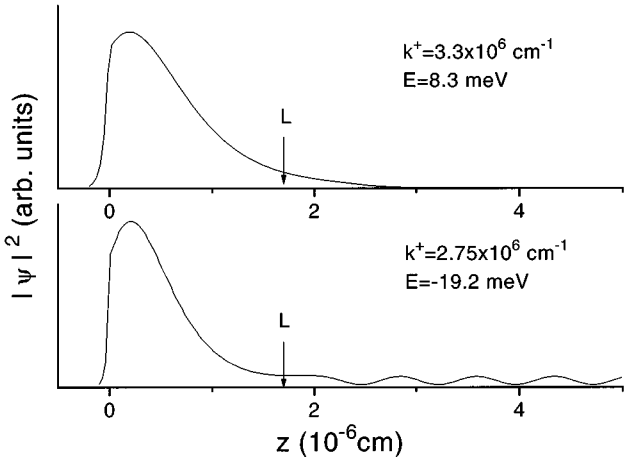

FIG. 15. $|\Psi|^2$ versus z curves for resonant (lower figure) and nonresonant (upper figure) 2D states. The parameters used are in the text.

$$g_{2D}\propto\frac{\int|\Psi(z)|^2dz}{A^2}, \qquad (15)$$

where A is the amplitude of $|\Psi|$ at $z>L$ and the integration runs over the space charge layer region.

Figure 16 shows the density of states corresponding to two groups of states, calculated for different values of quasimomentum k (in the following, k means k_y). It can be clearly seen that the width of the maxima rapidly increases with decreasing quasimomentum values. A peculiar feature is that the width of the maxima corresponding to the 0^+ branch is greater than that of the 0^- branch at the same energy. This means that the tunneling of 2D electrons to the valence band states is more effective for states of the 0^+ branch. At $k=0$ the 2D energy levels become well defined again.[33]

The dispersion law $E(k)$ of 2D electrons calculated for the described model with the above parameters is presented in Fig. 17. At $E>0$ the results coincide with those obtained without considering the remote bands. At negative energies when the 2D states are resonant, the energy levels are broad. This broadening is shown in Fig. 17 as hatched regions. The

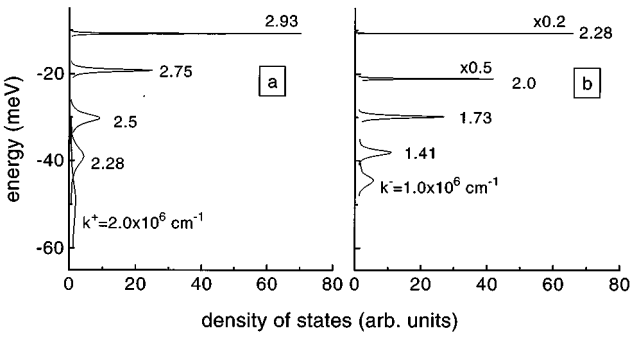

FIG. 16. The density of resonant 2D states for different quasimomentum values for 0^+ (a) and 0^- (b) branches.

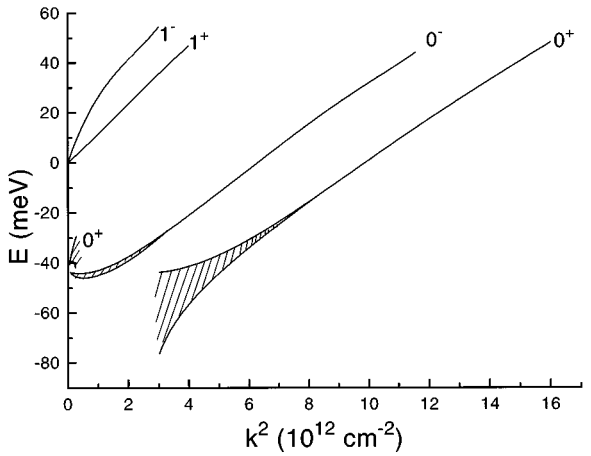

FIG. 17. The dispersion law of the 2D states localized in a surface quantum well. Two subbands split by spin-orbit interaction are shown. The hatched regions show the broadening of the 2D energy levels. The 2D states of the 0^+ branch are distroyed in the range $k^2=(0.3-3.0)\times10^{12}$ cm^{-2} due to the high probability of tunneling into the heavy hole states of the volume of the inverted semiconductor.

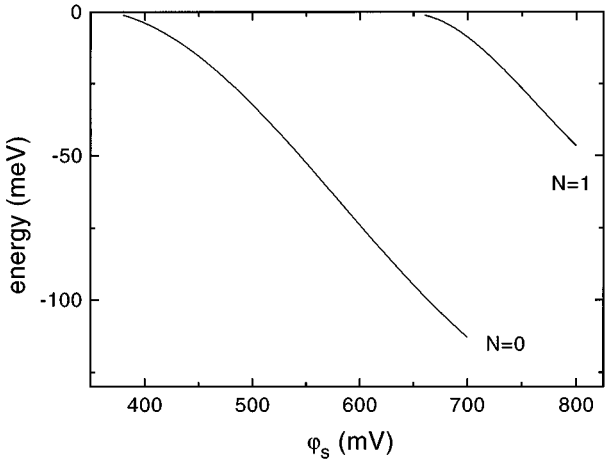

FIG. 18. The energy of the bottoms of the ground and first excited 2D subbands as a function of surface quantum well depth, calculated with parameters of structure 10-1.

width of these regions is defined here as the half width of the peak of the density of 2D states (see Fig. 16). In the narrow range of $k^2=(0.3-3)\times10^{12}$ cm^{-2}, the width of the density of states peak is very large, i.e., the 2D states are practically destroyed in this range.

Earlier, the resonance broadening of 2D states was discussed in Ref. 28 for narrow gap semiconductors and in Ref. 31 for semiconductors with an inverted spectrum. In these articles the tunneling to light hole states was taken into account, but tunneling to heavy hole states was neglected. In such an approximation the broadening of 2D states in inverted semiconductors occurs only at the energy less than E^{Γ_6} in the bulk of the semiconductor. As shown above, the tunneling to the heavy hole states is effective and this process has to be taken into account in inverted semiconductors.

VI. DISCUSSION

Let us begin with the discussion of experimental results obtained for the tunneling structures 10-1 to 11-1, based on heavily doped materials.

As mentioned above, there are two ways to understand the presence of two branches in the energy spectrum of the 2D states in the 10-1 structure. They are either ground and excited 2D subbands or two spin-split states of the ground 2D subband. The calculations carried out in the framework of the above model show (see Fig. 18) that as the surface potential increases, the excited subband at $k=0$ appears only when the energy of the ground subband is less than -100 meV (this value only slightly depends on the values of D_c and D_v). This is in contradiction with the experimental results presented in Fig. 6. Indeed, extrapolating the experimental curves to $k=0$ results in an energy difference between these branches that does not exceed 10 meV. Thus, these two branches of the 2D states are two spin branches of the 2D subband split by spin-orbit interaction.

For quantitative analysis of the experimental data, the parameters D_c, D_v, and bias dependence of φ_s should first be determined. The experimental results for the structures 10-1 to 10-6 provide a way of estimating the parameters D_c and D_v independent of $\varphi_s(V)$. In reality, we can calculate the φ_s relationships of the quasimomentum for the upper $k^-(\varphi_s)$ and lower $k^+(\varphi_s)$ branches of the 2D states at a fixed energy. Then eliminating φ_s we obtain a k^- versus k^+ dependence which is shown in the $\Delta(k^{+,-})^2$, $(k^+)^2$ coordinates in Fig. 9 for different values of D_c and D_v. The inspection of Fig. 9 shows that the results are not very sensitive to D_c and D_v as long as D_c and $D_v > E_g$ and $D_c \approx D_v$. But when $D_v > D_c$ and especially in the case when $D_v=\infty$, which corresponds to the zero boundary condition for the second component of the wave function, the results of the calculation significantly deviate from the experimental results. On first sight it seems to be surprising that the authors of Ref. 31 were able to explain the experimental results on the spin-orbit splitting of the 2D energy spectrum using such a boundary condition. An analysis of this article shows that this is due to using the approximate (quasiclassical) method of solving of eigenvalue problem in Ref. 31. Indeed, as is seen from Fig. 9, the results of the approximate calculations (dashed line) differ significantly from the exact solutions (line 4), but they are in better agreement with the experimental data.

Figure 9 shows that the more suitable parameters are $D_c=2$ eV, $D_v=1$ eV, and they will be used for the analysis of the results for all tunnel structures.

We have calculated the bias dependence of the quasimomentum of the lower spin branch over the entire bias range for structure 10-1, using the surface potential φ_s as a fitting parameter (inset in Fig. 6). With this $\varphi_s(V)$ relationship we have calculated the position of the upper spin branch of the 2D states (Fig. 6). One can see the good agreement with spin splitting over the whole energy range. Notice that at $k=0$ the energy of the 2D states coincides with the energy of the bottom of the conduction band, i.e., the binding energy of the 2D states at $k=0$ is equal to zero. This is a specific feature of the 2D states in an inverted semiconductor for weak quantum well strengths.

Curve 1 in Fig. 9 shows that the upper spin states must

disappear, when $\Delta(k^+)^2$ for the lower spin branch is less than 4×10^{12} cm^{-2}, which corresponds to a small surface potential $\varphi_s<230$ meV. Actually for the 10-3 to 10-6 structures only one spin branch exists over the whole energy range. This is illustrated by Fig. 10, which shows the energy versus quasimomentum curve for one of these structures (10-4). It can be clearly seen that the model employed describes the experimental data for these structures well.

Let us inspect the results for the structure 12-1 (Fig. 12). Contrary to structures of the first type (10-1 to 11-1), there are 2D electrons in this structure. Their concentration can be determined from the bias dependences of k^2 for oscillations of the second type (branches *a* and *b* in Fig. 12). The concentration is varied from $n_{2D}=1.3\times10^{12}$ cm^{-2} at $V=-60$ mV to $n_{2D}=1.0\times10^{12}$ cm^{-2} at $V=50$ mV. An estimation of the density of uncompensated acceptors in the space charge region gives a value of about 2×10^{12} cm^{-2}, which is of the same order of magnitude as n_{2D}; therefore the self-consistency of the potential has to be included in the calculation. Knowing the density of 2D electrons at different biases (see Sec. IV) and using a self-consistent procedure we have calculated the bias dependence of the surface potential (inset in Fig. 12). One can see that φ_s for the structure 12-1 is close to that of the structure 10-1 but due to the lower doping level (Table I) the width of the potential well is significantly larger, so that the strength of the potential well is also larger and more than one 2D subband is localized in such a well. Using this relationship between φ_s and bias we have calculated the quasimomenta of 2D states over the entire energy range (curves 1^+, 0^-, and 0^+ in Fig. 12). Curves *a* and *b* in Fig. 12 present the calculated values of the quasimomenta for both spin states at the energy $E=E_F$. As can be seen, there is good agreement for both types of oscillations over the whole bias range. Thus, both spin branches of the ground 2D subband and lower spin branch of the excited subband exist in the surface quantum well of this structure.

As was mentioned above (Sec. V), the 2D states should broaden at negative energy due to resonance with the valence band. This broadening is shown in Fig. 12 as well as in Fig. 17 by hatched regions. One can see that at the bias where oscillations were observed experimentally, broadening does not exceed 5 meV, i.e., it is less than the cyclotron energy in the investigated semiconductors at the magnetic fields, where oscillations were detected ($B>1$ T). With a more negative bias, the broadening becomes significantly larger and this is a possible reason why we do not observe oscillations at these biases.

Two comments are necessary in closing this section.

At first sight it may seem that the model of the insulator used for calculations of the energy spectrum of 2D states in our structures is forced. What actually happens is that this model imposes some relationships between the components of the wave function at the interface. Any insulator considered in the framework of the *kP* method imposes some relationships between the components too. The only point is, then, what relationships it imposes. In inverted and narrow gap semiconductors the amplitudes of all the components are about of the same value; therefore a widely used zero boundary condition for one of the components of the wave function[10,29–31] seems to be artificial.

All the experimental results on the energy spectrum of 2D states have been obtained from an analysis of oscillations of tunneling conductivity in a magnetic field, but the calculations were carried out without a magnetic field. For the comparison of the calculated results with the experimental data, the assumption was used that the quasiclassical rule for the quantization of the energy spectrum of 2D states in a magnetic field was fulfilled. To check this assumption, calculations of the Landau levels were also carried out. It was shown that except for the low surface potential values, when the energy difference between 2D and bulk states with the same quasimomentum was small, the quasiclassical rule for quantization in magnetic fields was fulfilled with good accuracy. Some results of these calculations and analysis of the peculiarities of the behavior of 2D Landau levels were discussed in Ref. 20.

VII. CONCLUSION

The energy spectrum of 2D states localized in a surface quantum well in an inverted semiconductor was studied by tunneling spectroscopy in a quantizing magnetic field. In the investigated structures the strength of the potential well mainly depends on the width of the well, which is controlled by the doping level: it increases when the acceptor concentration decreases. Two different cases were observed in our structures.

In the structures based on heavily doped material only the ground 2D subband exists and its bottom coincides with the bottom of the conduction band. Thus, in *p*-type material there are no 2D electrons and only empty 2D states exist. At $k\neq0$, the 2D ground subband is split by spin-orbit interaction. In structures with a larger potential well strength, both spin branches are observed, whereas in other structures the upper spin states are pushed into the continum and only the lower spin branch is observed.

In the structures based on materials with $N_A-N_D<10^{18}$ cm^{-3}, the strength of the potential well is so large that the ground and excited 2D subbands exist in these structures. In this case, both spin branches of the ground subband and only the lower spin branch of the excited subband are observed. In these structures the bottom of the ground subband lies significantly lower than the bottom of the conduction band and the 2D states are in resonance with the valence band over a wide energy range. The fact that oscillations relating to tunneling to such states are observed shows that the resonance broadening is not large and the 2D states are not destroyed at these energies.

Theoretical calculations carried out in the framework of the Kane model describe well all the peculiarities of the energy spectrum and spin-orbit splitting of 2D states in inverted semiconductors. Theoretical calculations which take the finite value of the heavy hole effective mass into account have shown that the broadening of 2D states due to resonance with the heavy hole valence band is large only over a narrow range of quasimomentum values. This is consistent with the results of our tunneling experiments.

ACKNOWLEDGMENTS

The authors would like to thank C. R. Becker for critically reading the manuscript, V. F. Radantsev for a copy of his work prior to publication, and V. Ya. Aleshkin for assistance in numerical calculations. This work was supported, in part, by the programme *Universities of Russia* and by a grant from the State Committee of the Russian Federation on Higher Education.

[1] M. I. Dyakonov and A. V. Khaetskii, Pis'ma Zh. Éksp. Teor. Fiz. **33**, 115 (1981) [JETP Lett. **33**, 110 (1981)].
[2] R. A. Suris, Fiz. Tekh. Poluprovodn. **20**, 2008 (1986) [Sov. Phys. Semicond. **20**, 1258 (1986)].
[3] Y. R. Lin-Liu and L. J. Sham, Phys. Rev. B **32**, 556 (1985).
[4] M. V. Kisin, Fiz. Tekh. Poluprovodn. **23**, 292 (1989) [Sov. Phys. Semicond. **23**, 180 (1989)].
[5] L. G. Gerchikov and A. V. Subashiev, Phys. Status Solidi B **160**, 443 (1990).
[6] C. A. Hoffman, J. R. Meyer, and F. J. Bartoli, Semicond. Sci. Technol. **8**, S48 (1993).
[7] J. R. Meyer, D. J. Arnold, C. A. Hoffman, and F. J. Bartoli, Phys. Rev. B **46**, 4139 (1992).
[8] G. M. Minkov, O. E. Rut, V. A. Larionova, and A. V. Germanenko, Zh. Éksp. Teor. Fiz. **105**, 719 (1994) [JETP **78**, 384 (1994)].
[9] Y. A. Bychkov and E. I. Rashba, J. Phys. C **17**, 6039 (1984).
[10] F. J. Ohkawa and Y. Uemura, J. Phys. Soc. Jpn. **37**, 1325 (1974).
[11] V. F. Radantsev, Zh. Éksp. Teor. Fiz. **96**, 1793 (1989) [Sov. Phys. JETP **69**, 1012 (1989)].
[12] R. Wollrab, R. Sizmann, F. Koch, J. Ziegler, and H. Maier, Semicond. Sci. Technol. **4**, 491 (1989).
[13] R. Sizmann and F. Koch, Semicond. Sci. Technol. **5**, S115 (1990).
[14] E. A. de Andrada e Silva, G. C. La Rocca, and F. Bassani, Phys. Rev. B **50**, 8523 (1994).
[15] G. L. Bir and G. E. Pikus, *Symmetry and Strain-Induced Effects in Semiconductors* (Wiley, New York, 1974).
[16] D. C. Tsui, Phys. Rev. B **8**, 2657 (1973).
[17] E. Böckenhoff, K. von Klitzing, and K. Ploog, Phys. Rev. B **38**, 10 120 (1988).
[18] J. Müller and U. Kunze, Semicond. Sci. Technol. **8**, 705 (1993).
[19] R. Winkler, U. Kunze, and U. Rössler, Surf. Sci. **263**, 222 (1992).
[20] G. M. Minkov, A. V. Germanenko, V. A. Larionova, and O. E. Rut, Semicond. Sci. Technol. **10**, 1578 (1995).
[21] D. C. Tsui, Phys. Rev. B **4**, 4438 (1971).
[22] L. P. Zverev, V. V. Kruzhaev, G. M. Minkov, and O. E. Rut, Zh. Éksp. Teor. Fiz. **80**, 1163 (1981) [Sov. Phys. JETP **53**, 595 (1981)].
[23] L. P. Zverev, V. V. Kruzhaev, G. M. Minkov, O. E. Rut, N. P. Gavaleshko, and V. M. Frasunyak, Fiz. Tverd. Tela **26**, 2943 (1984) [Sov. Phys. Solid State **26**, 1778 (1984)].
[24] A. V. Germanenko, G. M. Minkov, V. A. Larionova, O. E. Rut, C. R. Becker, and G. Landwehr, Phys. Rev. B **52**, 17 254 (1995).
[25] P. Bauernschmitt, J. Lindolf, and U. Kunze, Microelectron. Eng. **22**, 105 (1993).
[26] G. M. Minkov, A. V. Germanenko, V. A. Larionova, and O. E. Rut, Pis'ma Zh. Éksp. Teor. Fiz. **62**, 308 (1995) [JETP Lett. **62**, 330 (1995)].
[27] V. F. Radantsev, Semicond. Sci. Technol. **8**, 394 (1993).
[28] Pawel Sobkowicz, Semicond. Sci. Technol. **5**, 183 (1990).
[29] An-zhen Zhang, J. Slinkman, and R. F. Doezema, Phys. Rev. B **44**, 10 752 (1991).
[30] I. Nachev, Nuovo Cimento D **12**, 1143 (1990).
[31] V. F. Radantsev, T. I. Deryabina, G. I. Kulaev, and E. L. Rumyantsev, Phys. Rev. B **53**, 15 756 (1996).
[32] B. Freytag, U. Rössler, and O. Pankratov, Semicond. Sci. Technol. **8**, S243 (1993).
[33] R. Stepniewski, J. Phys. C **17**, L853 (1984).